JOURNAL OF CATALYSIS 132, 360–374 (1991)

Phase Cooperation between Tin and Antimony Oxides in Selective Oxidation of Isobutene to Methacrolein

III. Coprecipitated Catalysts

L. T. WENG, P. PATRONO,* E. SHAM, P. RUIZ, AND B. DELMON

*Unité de Catalyse et Chimie des Matériaux Divisés, Université Catholique de Louvain, Place Croix du Sud 1, 1348 Louvain-la-Neuve, Belgium; and *IMAI-CNR Aria, Ricerca, Via Salaria, CP 10 Monterolonctoscalo, Rome, Italy*

Received March 26, 1990; revised February 26, 1991

A series of Sb–Sn mixed oxides prepared by coprecipitation and calcined at high temperature (900°C) has been studied in the selective oxidation of isobutene to methacrolein. The catalytic properties of these samples depend strongly on the Sb content. The physico-chemical characterization using XRD, BET, electron microscopy (CTEM, SEM, and AEM), and XPS has shown that these samples are composed almost exclusively of a $Sb_xSn_{1-x}O_2$ solid solution and pure antimony oxide (Sb_2O_4). A strong catalytic synergy was observed when a Sb-poor coprecipitate was mixed with either a pure α-Sb_2O_4 or a Sb-rich coprecipitate. Physico-chemical characterization did not indicate any mutual contamination or the occurrence of solid state reaction. The catalytic performances of both pure coprecipitates and mechanical mixtures can be explained by a remote control mechanism, i.e., the fact that Sb_2O_4 produces spillover oxygen that can create or regenerate the selective catalytic sites of the $Sb_xSn_{1-x}O_2$ solid solution by reacting with its surface.

INTRODUCTION

Catalysts based on antimony and tin oxides are among the most efficient for olefin selective oxidation (*1*). Many scientific investigations have been devoted to this system and two excellent reviews have appeared in the literature (*2, 3*). It is usually agreed that, in order to be efficient, the catalyst should be subjected to high-temperature calcination and/or have a high Sb content. Made in this way, the catalysts contain several phases, among others a solid solution ($Sb_xSn_{1-x}O_2$) and an antimony oxide (α-β-Sb_2O_4, or Sb_6O_{13}). However, no general agreement has been reached with respect to many points such as the nature of active sites, the solubility of Sb in SnO_2, and the exact nature of the top layers on the surface for the samples with a low Sb content. Many postulates have been put forward to explain the origin of the active sites. These explanations can be roughly classified into four groups: (1) formation of the solid solution $Sb_xSn_{1-x}O_2$, as proposed by Godin *et al.* (*4*), Suzdalev *et al.* (*5*), and Crozat and Germain (*6*); (2) special arrangement of the cations at the surface, such as Sb^{3+} surrounded by Sn^{4+}, as proposed by Herniman *et al.* (*7*), Sn^{4+}–Sb^{3+} as acido-basic sites proposed by McAteer (*8, 9*), Sb(V)=O groups proposed by Sala and Trifirò (*10*), Sb^{5+}–Sb^{3+} pairs proposed by Benaichouba *et al.* (*11*) and special Sb arrangement such as in the (100) face of α-Sb_2O_4 proposed by Volta *et al.* (*12, 13*); (3) an oriented film of Sb_2O_4 supported on the surface of $Sb_xSn_{1-x}O_2$ solid solution proposed by Portefaix *et al.*(*14*); and (4) a bifunctional mechanism proposed by Ono *et al.* (*15*) and Halasz *et al.* (*16–18*). These divergent points of view are essentially coming from the complexity of the system, the difficulties encountered in its characterization, and the fact that different techniques

0021-9517/91 $3.00

(or even sometimes the same technique) lead to different interpretations. For example, it is usually agreed that the samples containing low Sb and calcined at high temperatures are enriched in Sb at the surface, as indicated by XPS (*19, 20*), but whether the top layers are segregated antimony oxide (*11–14*), amorphous antimony phases (*15, 21*), or constituted of specific Sn (IV)–Sb(III) arrangement (*7*) remains unclear.

Another point that has received less attention in the literature is the explanation of the role of antimony oxide in this system. This is mainly due to the fact that it is difficult to distinguish the contributions of $Sb_xSn_{1-x}O_2$, antimony oxide, and, possibly, SnO_2 to the overall activity. On the other hand, the fact that pure antimony oxide is almost inactive in allylic oxidation leads many investigators to neglect its role in real catalysis. This point deserves more attention because the catalysts possessing high selectivity are those in which antimony oxide is present. This should imply that it must play some important role in this Sn–Sb system.

The objective of this work is thus to try to contribute to the understanding of this system, particularly the role played by the various phases present. This is a continuation of the previous papers (*22, 23*) in which we have shown that there exists a strong cooperation between SnO_2 and α-Sb_2O_4 in the selective oxidation of isobutene to methacrolein. This is true not only in the case of the mechanical mixture (*22*) but also for catalysts prepared by impregnation of one cation on the oxide of the other (*23*). The explanation of the cooperation is that α-Sb_2O_4 produces spillover oxygen that migrates onto the surface of SnO_2 to improve its catalytic properties (by creating new selective sites and/or regenerating deactivated ones) (remote control mechanism). When SnSbO coprecipitates are considered, one may wonder whether the antimony oxide they contain plays a role similar to that of α-Sb_2O_4. In order to look into this point, we investigated whether the phases they contain could work synergetically as SnO_2 and Sb_2O_4 in the previous instances; we also used the same approach as in the previous studies, namely to study mechanical mixtures between the SbSnO coprecipitates (with different Sb contents) and α-Sb_2O_4. Mechanical mixing (actually making suspensions of the powders in *n*-pentane where the oxides are not soluble, mixing and drying) is used in order to avoid (or minimize) mutual contamination. If the presence of α-Sb_2O_4 in contact with coprecipitate is still a beneficial factor, this would confirm that separated α-Sb_2O_4 is necessary and would lead to the explanation of the role of this oxide in Sn–Sb catalysts. It is principally this problem that we examine.

There is another point that corresponds to the second aim of this paper. One could argue that mutual contamination explains the synergy between separate phases. We studied mechanical mixtures between two coprecipitates: one rich in Sn (called Sb-poor) and the other in Sb (called Sb-rich). In such a case, the underlying idea was to contaminate each phase with the other cation as extensively as possible from the start. If some cooperation still manifests itself, the only remaining explanation is cooperation between phases.

A third aim of our investigations concerns the careful characterization of the pure coprecipitates, especially those rich in Sb. Different points of view exist regarding the possible phases present in this region, e.g., Sn^{4+} dissolved in Sb_2O_4 (*24*), Sn^{4+}–Sb_2O_4 with pure Sb_2O_4 (*12–13*) and we hope to clarify some of these points.

EXPERIMENTAL

Catalyst Preparation and Characterization

α-Sb_2O_4 (2 m^2 g^{-1}) was prepared by calcination of Sb_2O_3 at 500°C for 20 h and is referred as Sb_2O_4(I). Mixed SbSnO oxides with different Sb contents (0, 1, 5, 8, 20, 40, 90, 95, 99, 100 at.%) were prepared by conventional coprecipitation of aqueous solutions of the respective chlorides ($SnCl_2$ ·

$2H_2O$, $SbCl_3 \cdot 3H_2O$) with ammonium hydroxide at pH 7, followed by filtering, washing for elimination of the Cl^- ions (and verification of elimination by $AgNO_3$), drying at 100°C overnight, and finally calcining at 900°C for 16 h. Hereafter, these coprecipitates are designated as S^x, where x refers to Sb content. As seen below, the coprecipitate may contain two phases: a solid solution and α-Sb_2O_4. The solid solution is designated as $Sb_xSn_{1-x}O_2$.

All the mechanical mixtures prepared contained identical weights (1 : 1) of the components. They were obtained by mixing and dispersing the respective powders in *n*-pentane for 10 min, evaporating the solvent, and drying at 80°C overnight. The mixtures were used as such (without calcination) in the catalytic experiments.

Fresh and used samples were characterized using XRD, BET, electron microscopy (CTEM, SEM, electron diffraction, and microanalysis (AEM)), and XPS techniques. The detailed description of these methods and data acquisition have been given in Parts I and II (*22, 23*). In the XPS measurements, we calculated, as described previously (*23*), the Sb XPS index, $r_{XPS\text{-}Sb}$ [Sb/(Sb + Sn)], representing approximately the fraction of surface developed by the phases containing Sb, using the sensitivity factors given by Wagner *et al.* (*25*). As in the previous studies (*22, 23*), the used samples were calcined in air at 400°C for 20 h to eliminate the coke formed during the reaction (regeneration). The binding energy values did not bring any valuable information for the reasons indicated previously (*22, 23*).

Catalytic Selective Oxidation of Isobutene

Selective oxidation of isobutene to methacrolein was carried out in a conventional fixed-bed reactor (*22*). The reactor and analysis systems have been described in detail in the previous articles (*22, 23*).

The catalyst was diluted with glass beads of similar size (500 μm) to reach a 1-cm height of catalytic bed. The reaction conditions were as follows: iso-$C_4H_8/O_2/N_2$ (diluting gas) = 1/2/7 (vol); total flow rate 60 ml/min; total pressure 760 mm Hg; and reaction temperature 420–460°C. The choice of reaction conditions, especially the catalyst weight (normally 300 mg; 150 mg with the highly active samples) was made in the same way as in Refs. (*22, 23*): the criteria were that a linear relation between conversion (and methacrolein yield) and catalyst weight existed and that the methacrolein yield was detectable for most samples. The experimental procedures were the same as in Part I (*22*).

TABLE 1

XRD Phases and Surface Areas of the Coprecipitate S^x

Sb content (%)	XRD phases	BET surface ($m^2\ g^{-1}$)
0	SnO_2	5.40[a]
1	SnO_2	8.49[a]
5	SnO_2	14.48[a]
8	SnO_2	10.92[a]
20	SnO_2 + α-Sb_2O_4 + β-Sb_2O_4	12.21[a]
40	SnO_2 + α-Sb_2O_4 + β-Sb_2O_4	8.98[a]
90	α-Sb_2O_4 + SnO_2	1.40[b]
95	α-Sb_2O_4 + SnO_2	1.00[b]
99	α-Sb_2O_4	0.60[b]
100	α-Sb_2O_4	0.60[b]

[a] Obtained by adsorption of N_2 at 77 K.
[b] Obtained by adsorption of krypton at 77 K.

RESULTS

PHYSICO-CHEMICAL CHARACTERIZATION

One part of the results for the samples concerning S^1 and S^5 have already been published (*26*). We recall only the essential points here.

1. Pure Coprecipitates

(a) XRD phases and BET surface areas. The crystallographic phases detected by XRD and the BET surface areas of the coprecipitated samples are reported in Table 1.

When the Sb content was lower than 8%, only SnO_2 was observed in XRD measure-

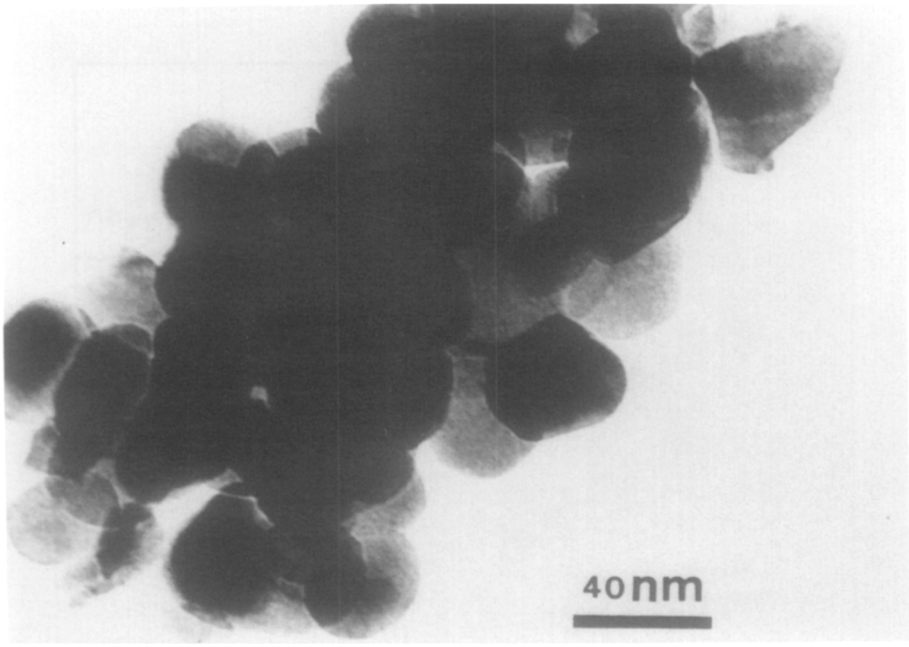

FIG. 1. CTEM micrograph for S^8.

ments. In the range of Sb% from 20 to 40, both SnO_2 and Sb_2O_4 phases (α with a small quantity of β) were obtained, but the peaks of Sb_2O_4 are much weaker than those of SnO_2. The relative intensity of Sb_2O_4 increases with the increase of nominal Sb content. The β-Sb_2O_4 was partially converted to α-Sb_2O_4 after reaction. In the Sb-rich region, α-Sb_2O_4 with a trace of SnO_2 was observed when the Sb content was <95 at.%; the relative intensity of the SnO_2 peaks increased with the decrease of Sb nominal content. Only α-Sb_2O_4 was detected in the samples containing 99 and 100 at.% of Sb.

The specific surface area passes through a maximum at 5 at.% of Sb. On the whole, the surface areas of the Sb-poor samples are larger than those of the samples rich in Sb.

(*b*) *Electron microscopy*. For the samples with a Sb content of less than 8 at.%, the particle size is about 30 nm on the average (Fig. 1 shows a typical CTEM micrograph for fresh S^8). Electron diffraction showed only the diffraction spots corresponding to SnO_2. AEM microanalysis indicated that both Sn and Sb signals appeared together and the ratio of Sn signal over Sb signal remained almost constant from one point to another and depended on the nominal Sb content in the samples.

The morphologies of most particles of S^{20} and S^{40} were similar to those of the samples with a Sb content lower than 8%. However, AEM showed that the Sb/Sn signal ratio varied from one analyzed point to another, i.e., that some parts were enriched in Sn, others in Sb. Only the electron diffraction patterns corresponding to SnO_2 were observed for either the region poor in Sb or the region rich in Sb. The diffraction spots characteristic of Sb_2O_4 (α or β) have never been detected. In some particular regions, we observed pure Sb oxide particles; the electron diffraction showed that these particles corresponded to Sb_2O_3. Figure 2 presents a CTEM micrograph and the corresponding AEM patterns for a particular analyzed region for fresh S^{40}. It should be stressed that very few regions of this kind were found in the samples.

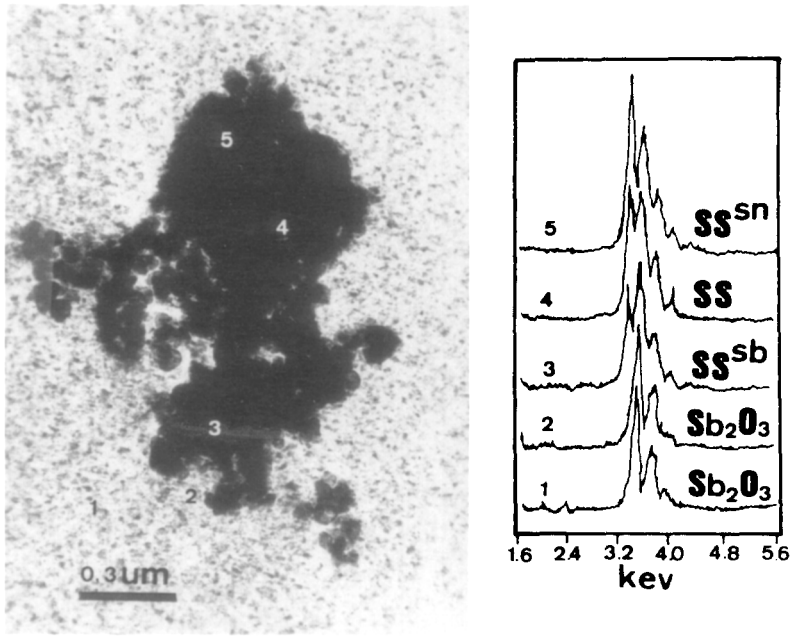

FIG. 2. CTEM micrograph and the corresponding AEM spectra for some special regions of S^{40} (see text); SS refers to solid solution.

For the Sb-rich samples, S^{90}, S^{95}, and S^{99}, observations by means of CTEM and SEM showed two kinds of particles, namely larger ones having smooth surfaces and smaller ones having morphologies similar to those observed above. The AEM microanalysis revealed that the former are pure Sb oxide and the latter contain both Sn and Sb. Figures 3 and 4 present a SEM micrograph for S^{95} and a CTEM micrograph with high amplification for S^{99}, respectively. The particle size of Sb oxide (larger particles) is comparable in all three samples, but slightly smaller than that in S^{100}. The particle size and Sb/Sn signal ratio of the smaller particles is almost comparable in all three samples, but the relative number of particles of each category depends on the nominal Sb content (decreasing with the increase of the Sb content). These particles are similar to those observed in Sb-poor samples.

After the catalytic reaction, no difference in any sample was noticed from the point of view of morphologies or particle size.

(*c*) *XPS.* Table 2 reports the XPS index, $r_{XPS\text{-}Sb}[Sb/(Sb + Sn)]$, for all coprecipitates S^x before and after the catalytic reaction and calcination at 400°C for 20 h. When the Sb content is low, the Sb/(Sb + Sn) ratio measured by XPS is greater than the nominal Sb content. This difference decreases with the increase of Sb content (e.g., $\approx$ 7.5 times greater for S^1, and only 1.5 times for S^{20}). For S^{40}, the $r_{XPS\text{-}Sb}$ index is almost equal to the nominal one. For the Sb-rich region, however, $r_{XPS\text{-}Sb}$ is small compared to the nominal Sb content; the extent of the difference is almost the same for all Sb-rich samples.

For all samples, the $r_{XPS\text{-}Sb}$ index remains constant after catalytic reaction and regeneration.

2. *Mechanical Mixtures of S^x with Sb_2O_4(I) and of the Sb-Poor Sample S^5 with Sb-Rich Samples*

(*a*) *X-ray diffraction.* Only the crystallographic phases characteristic of the starting

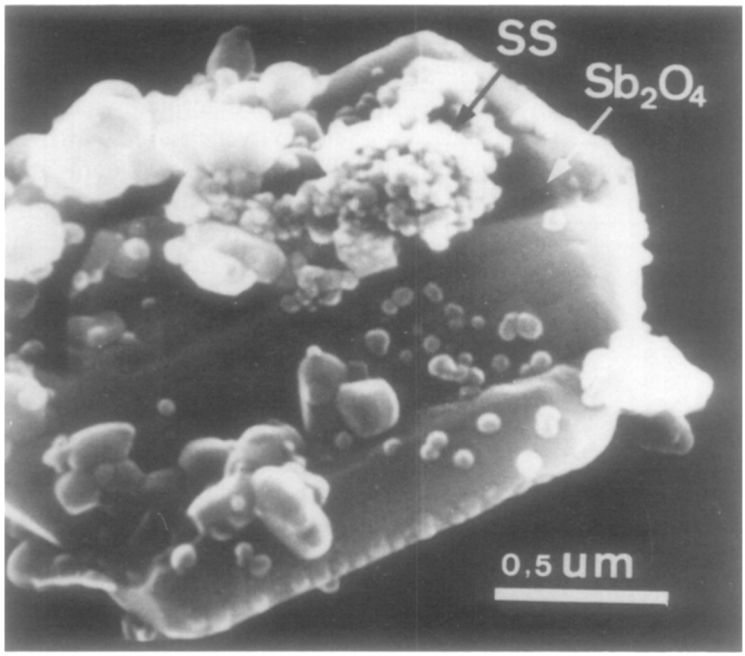

FIG. 3. SEM micrograph for S^{95}; SS refers to solid solution.

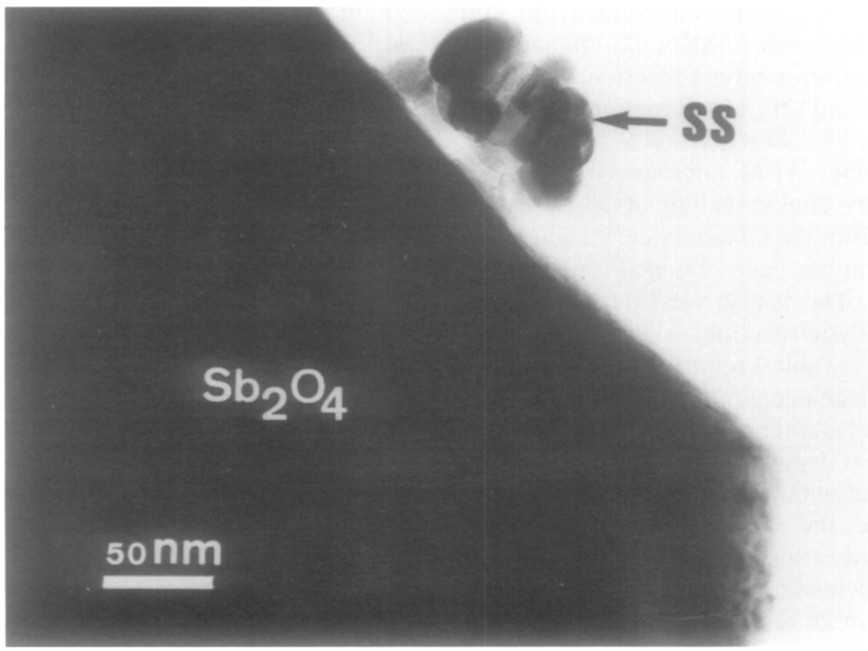

FIG. 4. CTEM micrograph for S^{99}; SS refers to solid solution.

TABLE 2

Sb Content Measured by XPS

Sb content (at.%)	r_{XPS-Sb}[Sb/(Sb + Sn)] (%)	
	Before reaction	After test + reg.[a]
0	0.0	0.0
1	7.6	7.8
5	21.4	21.9
8	31.8	31.8
20	32.9	32.9
40	35.9	36.2
90	72.6	73.1
95	79.7	80.1
99	96.1	95.8
100	100.0	100.0

[a] Reg. refers to the calcination of the sample at 400°C for 20 h.

oxides were observed. Compared with fresh samples, no change was observed for the used sample.

(*b*) *Electron microscopy.* The morphology and particle size of the mechanical mixtures were not changed in comparison with the starting oxides. Also, no change was observed after catalytic reaction. Figures 5 and 6 present CTEM micrographs for fresh mixtures, S^8 + Sb_2O_4(I) and S^{20} + Sb_2O_4(I), respectively. AEM microanalysis did not detect any contamination of Sb_2O_4 by Sn coming from the mixed oxide S^x. The same conclusion has been obtained for the other mixtures. This is also valid for the samples after catalytic reaction.

(*c*) *XPS.* Table 3 reports the r_{XPS-Sb} values for the mechanical mixtures S^x + Sb_2O_4(I) before and after catalytic reaction. Provided the carbon deposit is removed (present results), and within the precision limit of the technique, the r_{XPS-Sb} remained practically unchanged after catalytic reaction. The same conclusion was obtained for the mechanical mixtures of S^x poor in Sb with S^x rich in Sb, as shown in Table 4 (mechanical mixtures of S^5 with other S^x rich in Sb).

Catalytic Activity

1. Pure Coprecipitates

The methacrolein yield and methacrolein selectivity measured with the precipitates as a function of the Sb content at two reaction temperatures are presented in Figs. 7a and 7b respectively. The methacrolein yield passes through a maximum near 20 at.% of Sb. The activity of Sb-rich oxides (Sb% > 90%) is very low. For the samples poor in Sb, the methacrolein selectivity increases with the increase of Sb content. For the samples rich in Sb and having detectable activity, selectivity remains relatively high.

For S^1 and S^5, the increase of reaction temperature decreases the methacrolein selectivity substantially; the opposite effect is observed for the samples with Sb contents higher than 8 at.%.

2. Mechanical Mixtures S^x + Sb_2O_4(I)

In what follows, we must compare the results of the catalytic tests on our 1 : 1 (wt) mixtures with those that would be obtained by simply adding the effect due to the amount of each component *A* and *B* in the mixture, if they had worked alone. For this last calculation, we take advantage of the proportionality in isobutene conversion and in the yield of methacrolein in the experimental conditions that we have selected. Under these conditions, and 1 : 1 mixtures, the values $\overline{C}_{AB}$ or $\overline{Y}_{AB}$ taken for comparison are simply the average of the conversions (C_A and C_B) or yields (Y_A and Y_B) observed in our standardized test for components *A* and *B*. We have

$$\overline{C}_{AB} = \frac{1}{2}(C_A + C_B) \tag{1}$$

$$\overline{Y}_{AB} = \frac{1}{2}(Y_A + Y_B) \tag{2}$$

$$\overline{S}_{AB} = \frac{\overline{Y}_{AB}}{\overline{C}_{AB}} = \frac{Y_A + Y_B}{C_A + C_B}, \tag{3}$$

where *C*, *Y*, and *S* represent the conversion, yield, and selectivity, respectively.

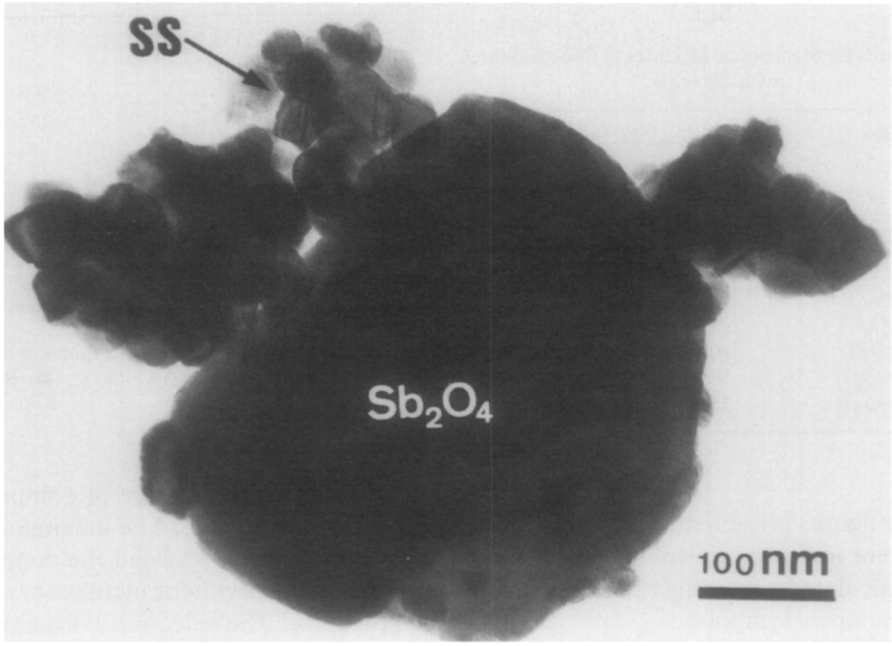

FIG. 5. CTEM micrograph for S^8 + Sb_2O_4(I); SS refers to solid solution.

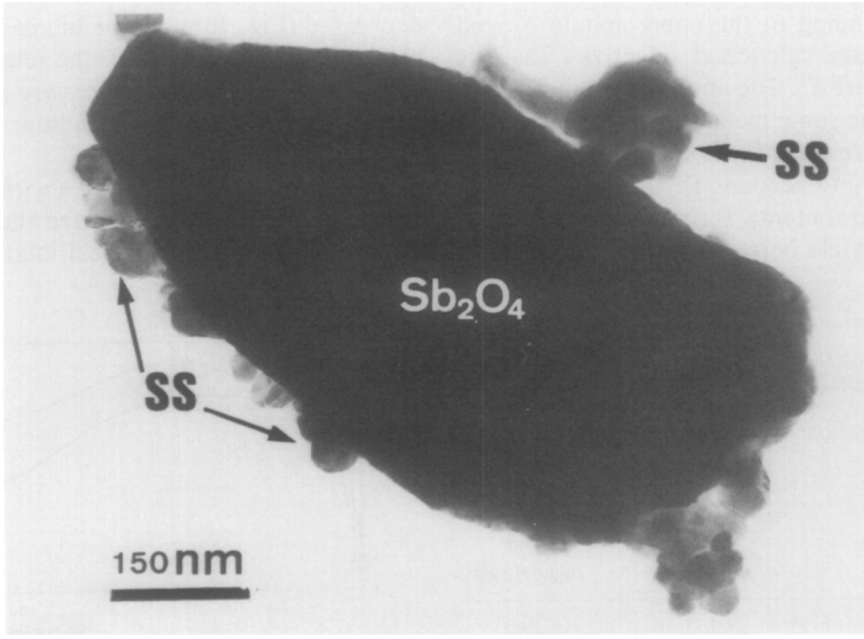

FIG. 6. CTEM micrograph for S^{20} + Sb_2O_4(I); SS refers to solid solution.

TABLE 3

XPS Results for Mechanical Mixtures of Coprecipitates with Sb_2O_4(I)

Samples	r_{XPS-Sb}[Sb/(Sn + Sb)]	
	Before test	After test and regeneration
S^1 + Sb_2O_4(I)	63.8	69.2
S^5 + Sb_2O_4(I)	41.8	45.3
S^8 + Sb_2O_4(I)	60.6	60.5
S^{20} + Sb_2O_4(I)	58.7	61.0
S^{40} + Sb_2O_4(I)	56.8	55.5

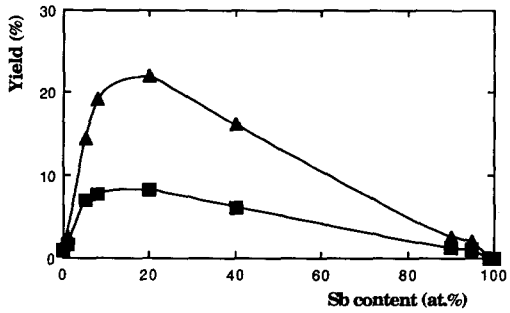

FIG. 7a. Methacrolein yield as a function of Sb content for the coprecipitates: (▲) 460°C, (■) 420°C.

In the figures presented, the experimental results are indicated by solid symbols, and those calculated according to the above formulas by open symbols.

(a) $S^x + Sb_2O_4(I)$. The methacrolein yield and selectivity of the mechanical mixtures of the various coprecipitates with Sb_2O_4(I) are presented in Figs. 8a and 8b, respectively. In this case, since α-Sb_2O_4 is inert, the average calculated yield ($\bar{Y}_{AB}$) is half that corresponding to the coprecipitate S^x and the average calculated selectivity ($\bar{S}_{AB}$) is that of pure S^x. The abscissa in Figs. 8a and 8b has the same meaning as in Figs. 7a and 7b: it represents the Sb content in S^x (we do not take into account Sb_2O_4(I) for calculating the Sb content). A cooperation for methacrolein yield between S^x and Sb_2O_4 is observed in the whole range of compositions investigated (Fig. 8a). The maximum cooperation is found for S^5 and the cooperative effect increases with the increase of reaction temperature. The selectivity observed with the mechanical mixtures of the precipitates S^x with Sb_2O_4 is higher than that of pure S^x. In absolute and relative values, the difference between them is higher for the S^x coprecipitates of low Sb content. It is interesting to note that the selectivities of S^1 and S^5 decreased (Fig. 7b) with the increase of the reaction temperature, while the selectivities of the corresponding mixtures are approximately independent of reaction temperature.

(b) Mixtures of S^x rich in Sn with S^x rich in Sb. In Ref. (*26*), we reported the results obtained with the mechanical mixtures of,

TABLE 4

XPS Results for the Mechanical Mixtures of S^5 and Sb-Rich Samples (*26*)

Samples	r_{XPS-Sb}[Sb/(Sn + Sb)] (%)	
	Before test	After test and regeneration
S^5 + S^{90}	35.0	39.0
S^5 + S^{95}	33.1	37.0
S^5 + S^{99}	36.8	40.0
S^5 + S^{100}	34.1	37.5

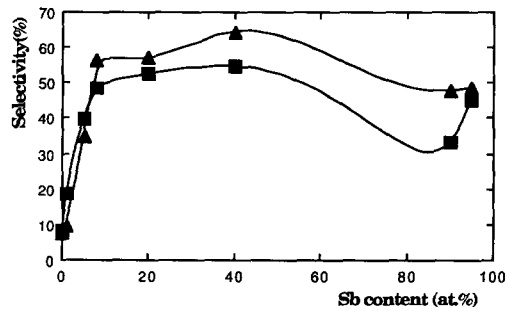

FIG. 7b. Methacrolein selectivity as a function of Sb content for coprecipitates at 420 and 460°C, respectively: (▲) 460°C, (■) 420°C.

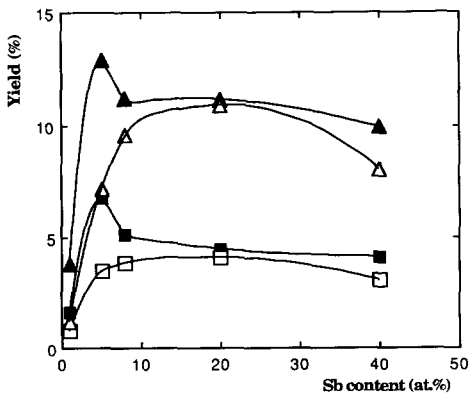

FIG. 8a. Methacrolein yield as a function of Sb content in S^x, for 1:1 (wt) mechanical mixtures S^x + Sb_2O_4(I) and yield calculated using Eq. (2), (■, ▲) experimental results; (□, △) values calculated with Eq. (2); (■, □) 420°C; (▲, △) 460°C.

on one hand, S^x poor in Sb (S^1 and S^5) and, on the other hand, S^x rich in Sb (S^{90}, S^{95}, S^{99} and S^{100}). It was shown that there existed a cooperation between these two kinds of solids, for both methacrolein yield and selectivity. The catalytic synergy increased with reaction temperature. With the same S^x poor in Sb, the catalytic synergy increased when the other phase contained more Sb. With the same S^x rich in Sb, the catalytic synergy increased when the other phase contained less Sb.

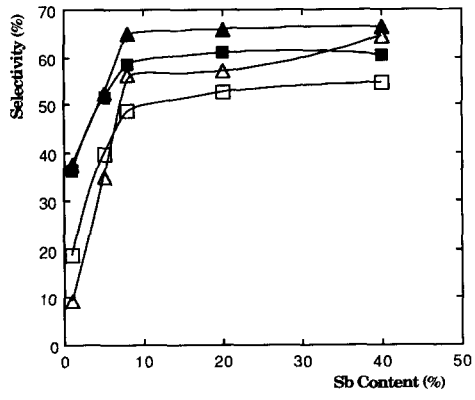

FIG. 8b. Methacrolein selectivity as a function of Sb content in S^x, for 1:1 (wt) mechanical mixtures S^x + Sb_2O_4(I), (■, ▲); and for the coprecipitates S^x (reference value) (□, △); (■, □) 420°C; (▲, △) 460°C.

DISCUSSION

Methacrolein yield and selectivity depend strongly on the content of Sb. The activity and selectivity of the Sb-poor samples can be improved by mixing them with either pure α-Sb_2O_4 or Sb-rich samples. The main objective of the discussion is to examine the different types of explanations concerning this catalytic synergy between two phases: formation of a new phase by reaction between the starting phases, surface contamination of one phase by the cation of the other, or mere physical contact of the two phases and role of spillover oxygen.

Possible Solid State Reaction between the Two Phases

1. Pure coprecipitates. For samples poor in Sb, namely $X < 8$ at.% Sb, XRD showed only the presence of solids with the SnO_2 structure. XPS showed an important enrichment of Sb at the surface and electron probe microanalysis indicated that the Sb/Sn ratio was constant from one particle to the other. All these results were similar to those reported in the literature (*2, 3, 12, 13, 19, 20*). These results and others obtained with other techniques, such as Mössbauer spectroscopy and electrical conductivity measurements, led to the generally accepted conclusion that Sb^{5+} ions can be incorporated into the SnO_2 lattice in a limited concentration for samples calcined at about 500–600°C (*2, 3*). When the calcination temperature increases, the Sb ions migrate to the surface. It has been suggested that when the Sb surface concentration is higher than a critical value, e.g., 25% according to the model proposed in Ref. (*20*), surface segregation of antimony oxide takes place. For samples similar to our S^5, careful studies by Mössbauer spectroscopy (*13*) and XPS technique have indicated the presence of this segregated oxide. Moreover, HREM (*21*) and XPS (*27*) have shown that this surface segregation can even occur during the catalytic

reaction, especially for samples that had not been subjected to high-temperature calcination.

Therefore, taking into account our own measurements and literature data, we can conclude that our S^1 is a solid solution $Sb_xSn_{1-x}O_2$ enriched with Sb at the surface (*26*). For the other samples, the quantity of antimony dissolved in SnO_2 should be low, of the order of 4–5 at.% (*3*), although Volta *et al.* (*12, 13*) have claimed a much higher solubility of Sb in SnO_2 (maximum 40%). The reason is that no measurable modification of the SnO_2 lattice was observed (no shift of the XRD lines was observed). If so, S^8 (and perhaps S^5) would be constituted of a solid solution with segregated antimony on the surface. This conjecture seems to be strongly confirmed by the XPS results of Table 2: with S^8, the Sb content $r_{XPS\text{-}Sb}$ at the surface reaches values (31.8%) comparable to those obtained with S^{20} (32.9%) or S^{40} (~36%). The already very high value (21–22%) observed for S^5 strongly suggests that Sb has also segregated at the surface to some extent. Although we cannot distinguish experimentally whether this segregated antimony oxide is in the form of a bidimensional layer (in epitaxy with $Sb_xSn_{1-x}O_2$) (*14, 19*) or a tridimensional oxide, we have arguments suggesting that it is likely to be a tridimensional oxide that forms on the surface. These reasons are the following: (i) for the samples containing more Sb, we observed a normal antimony oxide (α-Sb_2O_4) and particularly for those enriched in Sb, electron microscopy measurements indicated that the $Sb_xSn_{1-x}O_2$ and α-Sb_2O_4 particles are randomly in contact, as discussed below, and (ii) all these samples can benefit from the presence of α-Sb_2O_4 added simply by mechanical mixing, which suggests that epitaxy is not an indispensable condition.

For the samples S^{20} and S^{40} the XRD measurements showed the presence of antimony oxide (α with a trace of β-Sb_2O_4) in addition to the SnO_2 phase. However, electron diffraction was not able to detect pure Sb_2O_4 particles; the only particles that were detected in a few instances were pure Sb_2O_3. The fact that electron diffraction measurements could not detect the presence of the Sb_2O_4 phase may be explained by the fact that the phase is composed of very small crystallites and these crystallites are developed in random orientations (so the accumulation of the diffraction using a fixed analyzing angle, like in electron diffraction, is very small). On the other hand, AEM microanalysis shows that the Sb and Sn signals appear simultaneously and the Sb/Sn ratio differs from one analyzed zone to another: some parts of the catalyst are rich in Sb and others are rich in Sn. These results, in principle, may be compatible with the fact that the sample is a mixture of a solid solution $Sb_xSn_{1-x}O_2$ (with SnO_2 structure and rich in Sn) with a solid solution Sn^{4+}–Sb_2O_4 (with Sb_2O_4 structure and rich in Sb) or a mixture of a solid solutuion $Sb_xSn_{1-x}O_2$ with pure microcrystalline Sb_2O_4. The first possibility can be excluded by the fact that the contamination of Sb_2O_4 by Sn is impossible, as discussed below for the samples rich in Sb. Therefore, we can conclude that samples in the composition range S^{20}–S^{40} contain three phases: (i) a solid solution $Sb_xSn_{1-x}O_2$, (ii) Sb_2O_4 microcrystallites, and (iii) pure Sb_2O_3. It should be recognized that the presence of Sb_2O_3 is strange.It may be due to either the transformation of Sb_2O_4 (*24*) or the presence of some "isolated" Sb^{3+} ions during the catalyst preparation.

For the Sb-rich samples S^{90}, S^{95}, and S^{99}, two phases have been detected by XRD, namely α-Sb_2O_4 and traces of SnO_2. This is consistent with the observations by electron microscopy in which two kinds of particles have been observed, namely α-Sb_2O_4 and the $Sb_xSn_{1-x}O_2$ solid solution. This is true even with S^{99}, which contains only 1% Sn. These results mean that it is difficult or even impossible to form a solid solution of Sn in Sb_2O_4 or to contaminate the surface of Sb_2O_4 by Sn. This is not in agreement with the proposals in the literature (*12, 13, 24*), but it is totally in agreement with our results

presented previously for impregnated catalysts (*23*). In that study, we impregnated Sn ions over the surface of α-Sb_2O_4 in order, hopefully, to form a monolayer of SnO_2 over its surface, but the characterization results have shown that this artifically created contaminating layer disappeared during catalytic work.

In conclusion, for pure coprecipitates calcined at high temperatures (900°C in our case), the only solid solution formed is $Sb_xSn_{1-x}O_2$. When the Sb content increases, the mixed oxide is constituted of a pure $Sb_xSn_{1-x}O_2$ solid solution first (when Sb% < 5 at.%) and then a solid solution with segregated antimony oxide at the surface (5 at.% < Sb% < 40 at.%) and finally an antimony oxide with traces of $Sb_xSn_{1-x}O_2$ (Sb-rich sample). Although our measurements cannot prove it, it is natural to think that, in the last case, this $Sb_xSn_{1-x}O_2$ solid solution also carries Sb_2O_4 microcrystallites.

2. Mechanical mixtures. None of the physico-chemical measurements indicate that some solid state reaction or a surface contamination takes place in the mechanical mixtures. These results are quite logical. In fact, as discussed above, the pure coprecipitates have the tendency to segregate antimony oxide due to high-temperature calcination, especially in the case of Sb content higher than 5 at.%, rather than to become more enriched in antimony. Most of the starting coprecipitates already contained two phases. α-Sb_2O_4, on the other hand, has no tendency to become contaminated by Sn.

Explanation of the Catalytic Results

1. Mechanical mixture. When there is no mutual contamination between two starting oxides, the possible explanations for the catalytic synergy between these oxides are either a bifunctional mechanism or a remote control mechanism. The reasons for excluding the bifunctional mechanism have been given in the first paper of this series (*22*). The explanation we retain is thus the remote control mechanism.

According to the remote control mechanism applied to selective oxidation reactions, two kinds of roles should be distinguished: donors, D, produce spillover oxygen, and acceptors, A, possess potentially all the functions necessary for the selective catalysis, but they need to be irrigated by spillover oxygen. Antimony oxide α-Sb_2O_4 has practically no activity of its own: its only possible role is that of donor. The other phases, SnO_2 or the $Sb_xSn_{1-x}O_2$ solid solution, possess all the functions necessary for catalytic oxidation of isobutene, they are acceptors. In the present case, a complicating factor is that, for Sb contents equal to 5% or larger, microcrystallites of α-Sb_2O_4 are present on the surface of $Sb_xSn_{1-x}O_2$ solid solution, the donor action is exerted both by the individual, easily detected, α-Sb_2O_4 particles and by the microcrystallites supported on the $Sb_xSn_{1-x}O_2$ solid solution.

In the frame of the remote control mechanism, the role of spillover oxygen is to create new selective sites or to regenerate deactivated ones. The effect of adding α-Sb_2O_4 to coprecipitates must then be to increase the selectivity. This is exactly what is observed in catalytic activity results (Fig. 8b).

The fact that the magnitude of the catalytic synergy observed is higher with S^x containing low Sb when mixed with Sb_2O_4(I) can be explained by the fact that S^x with low Sb content has less or even no segregated antimony and therefore more Sb_2O_4 is needed. The same explanation can be given for the difference of catalytic synergy observed between S^x poor in Sb and S^x rich in Sb (*26*).

The effect of reaction temperature on selectivity is opposite for pure coprecipitates and their mechanical mixtures with α-Sb_2O_4. For S^1 (with no segregated Sb_2O_4) and S^5 (with only, possibly, a small amount of Sb_2O_4), the increase of reaction temperature decreases the selectivity (namely, favors the total oxidation). The effect ob-

served for the mechanical mixtures with Sb_2O_4(I) may be explained by the fact that the increase of reaction temperature favors the migration of spillover oxygen and thus increases the proportion of selective sites. Taking the same perspective, the fact that the selectivities of S^{20} and S^{40} increase with reaction temperature can be explained by the presence of segregated Sb_2O_4.

Another point discussed in Ref. (*26*) is that taking the same S^x poor in Sb (S^1 or S^5), we found that the catalytic synergy is higher with the pure Sb_2O_4(I) sample than with sample S^{100} although both are α-Sb_2O_4. In fact, the surface area of the former is higher and the particle size smaller than those of the latter. Thus more spillover oxygen can be produced with Sb_2O_4(I), and more contacts with S^x are possible, this increases the production and improves the efficiency of migration of spillover oxygen.

2. Pure coprecipitates S^x. Now let us examine whether the remote control mechanism can also explain the change of the catalytic activity of the pure S^x series with Sb content (Figs. 7a and 7b). Essentially, the $Sb_xSn_{1-x}O_2$ solid solution and antimony oxide (principally Sb_2O_4) are present in these coprecipitates. The difference between the various samples of the series would come from the difference of the quantity, dispersion, and surface areas of these two phases. As shown above, pure Sb_2O_4 is inactive. Thus the activity of the coprecipitate will come directly from $Sb_xSn_{1-x}O_2$ solid solution. According to the remote control mechanism, the catalytic performance of this solid solution would depend strongly on the "degree" of the activation of this phase by spillover oxygen emitted by Sb_2O_4. Ideally, we should compare activities (methacrolein yield) per unit surface area of the potentially active phase (intrinsic activity). However, it is difficult to estimate the surface area developed by the solid solution when antimony oxide is also present. In an approximation, we calculated the intrinsic yield, namely yield-to-surface area ratio, by dividing the yield by the *total* surface area of each sample. The results are reported in Fig. 9. The intrinsic yield increases quickly with Sb content when Sb% < 8 at.% and then remains almost constant. In the way we make the calculations, we underestimate the intrinsic yield when the coprecipitates contain antimony oxide (which develops a surface area of its own) for Sb contents higher than 8%. The increase of intrinsic yield is thus actually larger than the curves in Fig. 9 indicate. This increase is consistent with the prediction by the remote control mechanism.

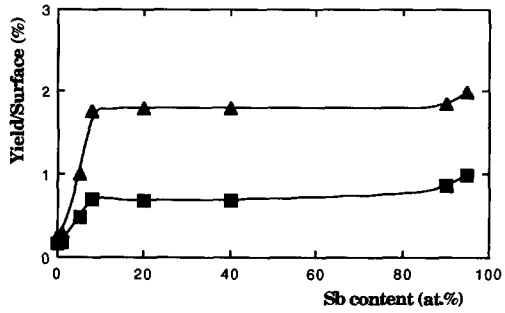

FIG. 9. Intrinsic activity (yield/surface area) for the coprecipitates (▲) 460°C, (■) 420°C.

CONCLUSIONS

- The catalytic performances in the selective oxidation of isobutene of pure Sb–Sn coprecipitates calcined at high temperatures depend strongly on the Sb content. The principal phases present in these oxides are a $Sb_xSn_{1-x}O_2$ solid solution and antimony oxide (Sb_2O_4).
- A conspicuous synergy is observed between a coprecipitate poor in Sb with either pure Sb_2O_4 or a coprecipitate rich in Sb.
- The catalytic activity results of either pure coprecipitates or mechanical mixtures can be explained by a remote control mechanism.

The general conclusions drawn from the work described in Parts I, II, and III are that in the Sb–Sn catalytic system, the stable phases are SnO_2 or an antimony-poor

$Sb_xSn_{1-x}O_2$ solid solution and antimony oxide (most often Sb_2O_4) and that the catalytic performances of the catalysts in isobutene oxidation can be satisfactorily explained by a remote control mechanism. Based on this mechanism, the methacrolein yield and the selectivity depend strongly on the activation of SnO_2 or the $Sb_xSn_{1-x}O_2$ solid solution by antimony oxide. We can thus expect that a good catalyst should be one containing SnO_2 or $Sb_xSn_{1-x}O_2$ and Sb_2O_4, both highly dispersed and in intimate contact. This explains why the coprecipitated samples containing low Sb content should be calcined at high temperature (in order to obtain antimony oxide segregated at surface). However, the disadvantages of this preparation method is that a high-temperature calcination causes extensive sintering of the sample and a loss of surface area. Another way to obtain segregated antimony is to use larger amounts of Sb in the formulation, but this brings about the formation of large Sb_2O_4 particles, decreasing the number of contacts with SnO_2 or the $Sb_xSn_{1-x}O_2$ solid solution. It is desirable to use a preparation method that produces small Sb_2O_4 particles in excellent contact with the SnO_2 or $Sb_xSn_{1-x}O_2$ and to protect the phases against sintering. Low-temperature preparations, in particular those using impregnations, seem to have a potential for giving very efficient catalysts.

ACKNOWLEDGMENTS

We gratefully thank the Université Catholique de Louvain and the Chinese Government for financial support of one of us (L. T. Weng), and the Service de Programmation de la Politique Scientifique for supporting this line of research in our laboratory. We also acknowledge the financial support of NATO for the stay of P. Patrono in Louvain-la-Neuve. We thank Dr. J. Naud for his help in XRD measurements.

REFERENCES

1. Bethell, J. R., and Hadley, D. J., U.S. Patent, 3,094,565 (1963); Barclay, J. L., Bethell, J. R., Bream, J. B., Hadley, D. J., Jenkins, R. H., Stewart, D. G., and Wood, B., British Patent, 864,666 (1960).
2. Berry, F. J., *in* "Advances in Catalysis" (D. D. Eley, H. Pines, and P. B. Weisz, Eds.), Vol. 30, p. 97. Academic Press, New York, 1980.
3. Viswanathan, B., and Chokkalingam, S., *Surf. Technol.* **26,** 231 (1984).
4. Godin, G. W., McCain, C. C., and Porter, E. A., *in* "Proceedings, 4th International Congress on Catalysis, Moscow, 1968" (B. A. Kazansky, Ed.), Vol. 1, p. 347, Adler, New York, 1968.
5. Suzdalev, I. P., Firsora, A. A., Alexandrov, A. V., Morgolis, L. Ya., and Baltrunas, D. A., *Dokl. Akad. Nauk. SSSR* **204,** 408 (1972).
6. Crozat, M., and Germain, J. E., *Bull. Soc. Chim. Fr.*, 1125 (1973).
7. Herniman, H. J., Pyke, D. R., and Reid, R. J., *J. Catal.* **58,** 68 (1979).
8. McAteer, J. C., *J. Chem. Soc. Faraday Trans. 1* **75,** 2762 (1979).
9. McAteer, J. C., *J. Chem. Soc. Faraday Trans. 1* **75,** 2768 (1979).
10. Sala, F., and Trifirò, F., *J. Catal.* **34,** 68 (1974).
11. Benaichouba, B., Bussière, P., Friedt, J. M., and Sanchez, J. P., *Appl. Catal.* **8,** 237 (1983).
12. Volta, J. C., Benaichouba, B., Mutin, I., and Védrine, J. C., *Appl. Catal.* **8,** 215 (1983).
13. Volta, J. C., Bussière, P., Coudurier, C., Herrmann, J. M., and Védrine, J. C., *Appl. Catal.* **16,** 315 (1985).
14. Portefaix, J. L., Bussière B., Forissier, M., Figueras, F., Friedt, J. M., Sanchez, J. P., and Théobald, F., *J. Chem. Soc., Faraday Trans. 1* **76,** 1652 (1980).
15. Ono, T., Yamanaka, T., Kubokawa, Y., and Komiyama, M., *J. Catal.* **109,** 423 (1988).
16. Halasz, J., Varga, K., Fejes, P., and Hernadi, K., *Acta Chim. Hungar.* **124,** 35 (1987).
17. Halasz, J., Varga, K., Fejes, P., Laszlo, J., and Hernadi, K., *Appl. Catal.* **34,** 135 (1987).
18. Halasz, J., Varga, K., and Fejes, P., *J. Mol. Catal.* **51,** 303 (1989).
19. Boudeville, Y., Figueras, F., Forissier, M., Portefaix, J. L., and Védrine, J. C., *J. Catal.* **58,** 52 (1979).
20. Cross, Y. M., and Pyke, D. R., *J. Catal.* **58,** 61 (1979).
21. Smith, D. J., Bursill, L. A., and Berry, F. J., *J. Solid State Chem.* **44,** 326 (1982); Berry, F. J., and Smith, D. J., *J. Catal.* **88,** 107 (1984).
22. Weng, L. T., Spitaels, N., Yasse, B., Ladrière, J., Ruiz, P., and Delmon, B., *J. Catal.* **132,** 319 (1991).
23. Weng, L. T., Yasse, B., Ladrière, J., Ruiz, P., and Delmon, B., *J. Catal.* **132,** 343 (1991).
24. Roginskaya, Yu. E., Dulin, D. A., Stroeva, S. S., Kul'kova, N. V., and Gel'bshtein, A. I., *Kinet. Katal.* **9,** 1143 (1968).

25. Wagner, C. D., Davis, L. E., Zeller, H. V., Taylor, P. A., Raymond, R. H., and Gale, L. H., *Surf. Interface Anal.* **3,** 21 (1981).
26. Weng, L. T., Patrono, P., Sham, E., Ruiz, P., and Delmon, B., *in* "New Developments in Selective Oxidation" (G. Centi and F. Trifirò, Eds.), p. 797. Elsevier, Amsterdam, 1990.
27. Viswanathan, B., Chokkalingam, S., Varadarajan, T. K., and Badrinarayanan, S., *Surf. Coating Technol.* **28,** 201 (1986).